

## IRON AND RUTHENIUM COMPLEXES

**[M<sub>2</sub>(CO)<sub>6</sub>(PYRIDINE-2-CARBALDEHYDE-IMINE)] HAVING A σ-N, μ<sub>2</sub>-N', η<sup>2</sup>-C=N' BONDED 6-R<sup>1</sup>-py-2-C(R<sup>2</sup>)=NR LIGAND; X-RAY STRUCTURE OF [Ru<sub>2</sub>(CO)<sub>5</sub>{1,2-BIS(μ-ISOPROPYLAMIDO)-1,2-BIS(2-PYRIDYL)ETHANE}] CONTAINING TWO C–C LINKED PYRIDINE-2-CARBALDEHYDE-IMINE LIGANDS**

LOUIS H. POLM, GERARD VAN KOTEN, CORNELIS J. ELSEVIER, KEES VRIEZE\*,

*Anorganisch Chemisch Laboratorium, University of Amsterdam, Nieuwe Achtergracht 166, 1018 WV Amsterdam (The Netherlands)*

BERNARD F.K. VAN SANTEN and CASPER H. STAM

*Laboratorium voor Kristallografie, University of Amsterdam, Nieuwe Achtergracht 166, 1018 WV Amsterdam (The Netherlands)*

(Received October 21st, 1985)

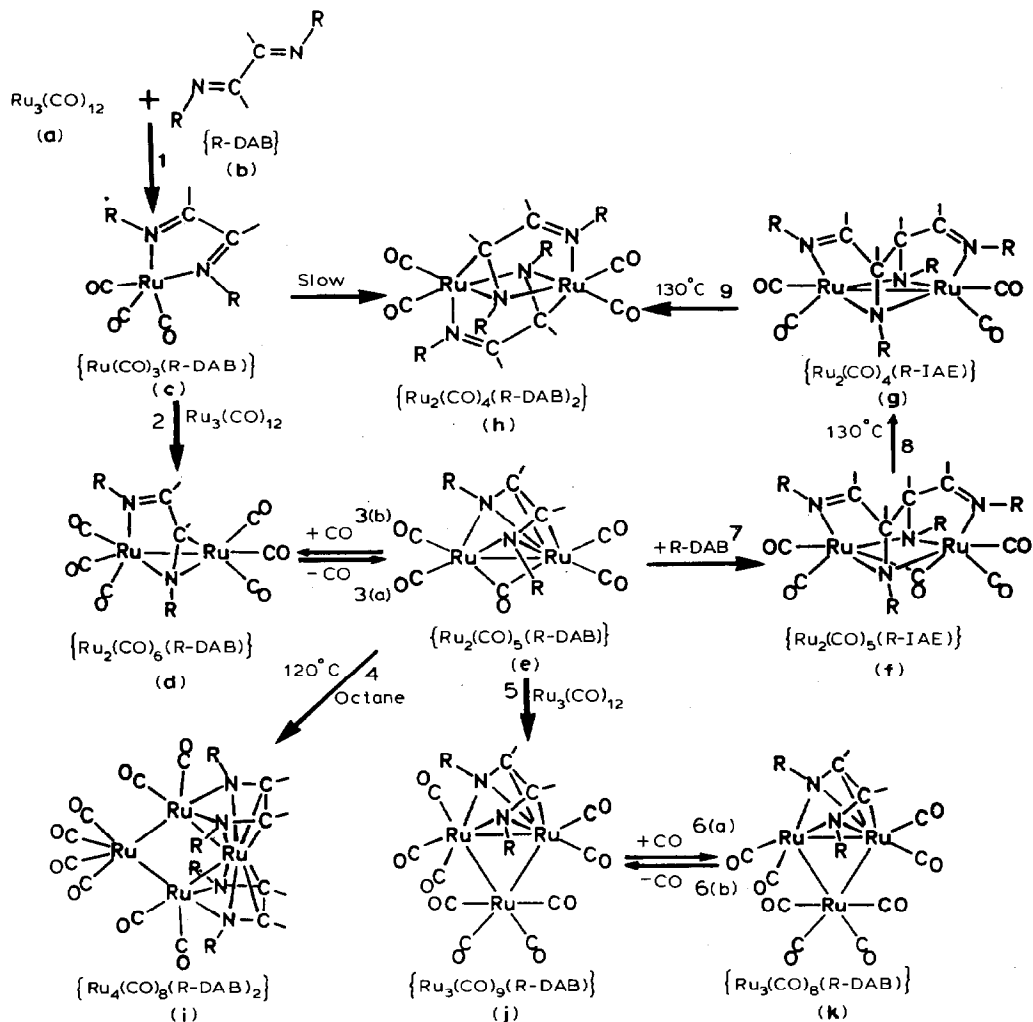
### Summary

The pyridine-2-carbaldehyde-imines R<sup>1</sup>-py-2-C(R<sup>2</sup>)=NR (R-Pyca) react with Fe<sub>2</sub>(CO)<sub>9</sub> to give Fe<sub>2</sub>(CO)<sub>6</sub>(R-Pyca) and Fe(CO)<sub>3</sub>(R-Pyca) and with Ru<sub>3</sub>(CO)<sub>12</sub> to Ru<sub>2</sub>(CO)<sub>6</sub>(R-Pyca). Further reaction of Ru<sub>2</sub>(CO)<sub>6</sub>(R-Pyca) with R-Pyca gives Ru<sub>2</sub>(CO)<sub>5</sub>(R-APE)(R-APE = 1,2-bis(μ-alkylamido)-1,2-bis(2-pyridyl)ethane), in which R-APE consists of two C–C linked R-Pyca ligands.

One representative Ru<sub>2</sub>(CO)<sub>5</sub>(R-APE) compound, viz. that with R = i-Pr, has been studied by X-ray diffraction. The compound Ru<sub>2</sub>(CO)<sub>5</sub>(i-Pr-APE) is monoclinic, space group *P2<sub>1</sub>/n* with two molecules in a unit cell of dimensions *a* 14.499(5), *b* 9.051(3), *c* 9.772(4) Å and β 103.54(4)°; *Z* = 2, *R* = 0.057 for 1743 observed reflections. Although the crystals were not of sufficient quality to warrant detailed discussion of the structure, it is clear that the 10e donor APM ligand bridges the Ru<sub>2</sub>(CO)<sub>5</sub> unit in which there is no Ru–Ru bond. <sup>1</sup>H and <sup>13</sup>C NMR data for the free ligands and their Fe and Ru complexes are discussed, with emphasis on π-backbonding from the Group VIII metal to the imine C=N' bond.

### Introduction

Extensive investigations of reaction systems containing Ru<sub>3</sub>(CO)<sub>12</sub> and R-DAB (R-DAB = RN=C(H)–C(H)=NR is a 1,4-disubstituted-1,4-diaza-1,3-butadiene) have shown that depending on the steric bulk of R, i.e. on the way the C=N bonds are



SCHEME 1. Reactions occurring in the system  $\text{Ru}_3(\text{CO})_{12}/\text{R-DAB}$ . The pathway chosen depends on R and the concentrations of reagents present in solution. Products c–k isolated from the reactions 1–9 in which R (c–k): c: R = 2,4-dimethylpent-3-yl; 2,4,6-Mesityl; 2,6-xylyl [1], d: R = t-Bu; i-Pr; c-Hex [2], e: R = i-Pr; c-Hex; neo-Pent; i-Bu [3], f: R = t-Bu; i-Pr; c-Hex [2], g: R = i-Pr; c-Hex [2], h: R = i-Pr; c-Hex; *p*-Tol [2], i: R = i-Pr; c-Hex [1], j: R = c-Hex; neo-Pent; i-Bu [1,4], k: R = c-Hex; neo-Pent; i-Bu [1,4,5].

protected against further coordination by a metal atom, different products may predominate (see Scheme 1).

The proposed reaction scheme involves an initial complete breakdown of  $\text{Ru}_3(\text{CO})_{12}$  to mononuclear  $\text{Ru}(\text{CO})_3(\text{R-DAB})$  (reaction 1) containing a  $4e \sigma, \sigma\text{-N}, \text{N}'$ -donor ligand. Depending on R, the reaction may then continue with the formation of  $\text{Ru}_2(\text{CO})_6(\text{R-DAB})$  (reaction 2), which possesses a  $6e \sigma\text{-N}, \mu\text{-N}', \eta^2\text{-C}=\text{N}'$  donor R-DAB group, and subsequently of  $\text{Ru}_2(\text{CO})_5(\text{R-DAB})$  (reaction 3a), in which the R-DAB ligand now acts as a  $8e \sigma\text{-N}, \sigma\text{-N}', \eta^2\text{-C}=\text{N}, \eta^2\text{-C}=\text{N}'$  donor.

$\text{Ru}_2(\text{CO})_5(\text{R-DAB})$  appears to be a key-intermediate in this system since it reacts (a) with CO to give  $\text{Ru}_2(\text{CO})_6(\text{R-DAB})$  (reaction 3b), (b) when heated on its own to

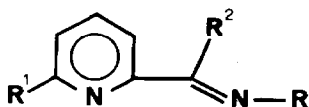


Fig. 1. Schematic structure of R-Pyca{R<sup>1</sup>, R<sup>2</sup>} ligand.

give Ru<sub>4</sub>(CO)<sub>8</sub>(R-DAB)<sub>2</sub> (reaction 4), and (c) when heated with Ru<sub>3</sub>(CO)<sub>12</sub> to give Ru<sub>3</sub>(CO)<sub>9</sub>(R-DAB) (reaction 5). In the last two products the R-DAB ligand is bonded in the 8e bonding mode. Ru<sub>3</sub>(CO)<sub>9</sub>(R-DAB) may be converted into Ru<sub>3</sub>(CO)<sub>8</sub>(R-DAB) (reaction 6a) by CO elimination, for example in a N<sub>2</sub> atmosphere, and the reverse reaction (6b) takes readily place upon addition of CO to the latter product [4]. Finally, reactions of Ru<sub>2</sub>(CO)<sub>5</sub>(R-DAB) with free R-DAB (reactions 7, 8) under N<sub>2</sub> give rise to a very interesting C–C coupling reaction with the formation of Ru<sub>2</sub>(CO)<sub>n</sub>(IAE)\* (*n* = 4, 5).

In some cases, depending on R, the latter product could not be isolated, because it was converted directly into Ru<sub>2</sub>(CO)<sub>4</sub>(R-DAB)<sub>2</sub> (reactions 3, 7, 8, 9) containing two 6e donor R-DAB ligands. The latter complex is formed as a result of a cleavage of the C–C bond formed in the preceding reaction [2].

In particular the C–C coupling (and decoupling) reactions attracted our interest, since such reactions have not only been observed between two R-DAB ligands, but also between R-DAB and either alkynes or pseudoallenes (e.g.: RN=C=NR or R<sub>2</sub>C=S=O) [6]. In order to investigate the chemistry of the complexes M<sub>2</sub>(CO)<sub>6</sub>(α-diimine) in general, and in particular to study the subsequent C–C coupling and decoupling reactions in more detail, we examined the analogous reactions of Ru<sub>3</sub>(CO)<sub>12</sub> with the R-Pyca{R<sup>1</sup>, R<sup>2</sup>} ligand \*\* (Fig. 1).

For the latter type of α-diimine ligand a change of the reaction pattern was expected for the following reasons:

(i) The 8e-coordination mode will be very unlikely because of the resonance stabilization of the pyridine ring, which would then effectively block reactions 4 and 5 (see Scheme 1).

(ii) Our recent observations on the reactions of R-DAB and R-Pyca ligands with organozinc reagents included detection of a rather unusual C–C bond formation, as shown in Fig. 2. This equilibrium involves a C–C (de)coupling reaction of two three-coordinate [EtZn(α-diimine)] radicals in which α-diimine is either R-DAB or R-Pyca. The molecular geometry of one of these dimers, viz. Et<sub>2</sub>Zn<sub>2</sub>(t-Bu-APE) [7] (R-APE = bis(alkylamido)bis(2-pyridyl)ethane), in the solid state has been established, and is schematically shown in Fig. 2. The C–C coupled diimine appeared to be more stable for R-Pyca than for R-DAB with respect to dissociation into the respective monomers.

(iii). So far the C–C coupling reaction 7 has only been observed in the case of the Ru<sub>3</sub>(CO)<sub>12</sub>/R-DAB system. All attempts to bring about similar reactions with iron carbonyls failed. However, such C–C coupling reactions should be feasible in principle; thus Weiss et al. [8] reported that Fe<sub>2</sub>(CO)<sub>9</sub> reacts with O=C(OEt)-C(H)=NPhC(H)(Me) (= L) to give Fe<sub>2</sub>(CO)<sub>6</sub>L and Fe<sub>2</sub>(CO)<sub>6</sub>L<sub>2</sub>, and Frühauf et al.

\* IAE = 1,2-bis(alkylimino)-1,2-(alkylamino)ethane.

\*\* The abbreviation R-Pyca is used generally to denote the ligand with its various substituents unspecified.

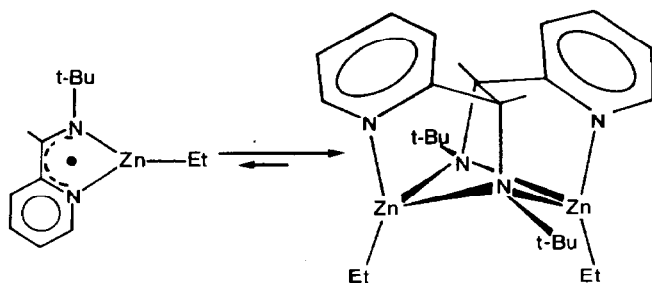


Fig. 2. Equilibrium between the radical  $[ZnEt(t-Bu-Pyca)]^\cdot$  and the C-C coupled dimer  $Zn_2Et_2(t-Bu-APE)$ .

recently showed that in the presence of an excess of CO, C-C coupling reactions can be induced at R-DAB ligands coordinated to Fe [9].

In this paper we direct our attention to a discussion of the formation of  $M_2(CO)_6(R-Pyca)$  ( $M = Fe, Ru$ ) containing 6e bonded R-Pyca as well as to a reaction involving C-C bond formation. The crystal structure of  $Ru_2(CO)_5(i-Pr-APE)$ , which contains two C-C linked R-Pyca ligands, is presented. In a later article the use of an excess of CO to influence the C-C (de)coupling reaction will be discussed [10].

## Experimental

### Materials and apparatus

The  $^1H$  NMR spectra were recorded on a Varian T 60 or a Bruker WM 250 and the  $^{13}C$  spectra on a Bruker WP 80 spectrometer. IR spectra were recorded with a Perkin-Elmer 283 spectrophotometer. Mass spectra were obtained with a Varian MAT 711 spectrometer by use of the Field Desorption Technique [11]. Elemental analyses were carried out by the section Elemental Analyses of the Institute for Applied Chemistry TNO, Zeist (The Netherlands) (see Table 1).

All preparations were carried out in an atmosphere of purified nitrogen, using carefully dried solvents. Silica-gel for column chromatography (60 mesh) was purchased from Merck and heated at  $180^\circ C$  under vacuum overnight before use.  $Ru_3(CO)_{12}$  was purchased from Strem Chemicals (U.S.A.) and was used without further purification.  $Fe_2(CO)_9$  was prepared by irradiating  $Fe(CO)_5$  with UV light in a glacial acetic acid and acetic acid anhydride mixture under nitrogen [12]. The pyridine-2-carbaldehyde-imine ligands were prepared by published methods [13-15].

### Preparation of $Fe_2(CO)_6(R-Pyca\{R^1, R^2\})$ with ( $R^1 = H, Me; R^2 = H; R = t-Bu, i-Pr, c-Hex, i-Bu, p-Tol, 2,4,6-Mes$ (I-XII))

The complexes  $Fe_2(CO)_6(R-Pyca\{R^1, R^2\})$  with ( $R-Pyca\{R^1, R^2\} = R$ -pyridine-2-carbaldehydeimine) were prepared by refluxing a solution of 3 mmol of  $Fe_2(CO)_9$  and the relevant pyridine-imine ligand in a 3/1 molar ratio in 75 ml of n-hexane at  $70^\circ C$ . The reaction was monitored with IR ( $\nu(CO)$  region), and was stopped when the intensities of the characteristic IR bands of the dimeric compound had reached a maximum. The presence of  $Fe_2(CO)_6(R-Pyca\{R^1, R^2\})$ ,  $Fe(CO)_3(R-Pyca\{R^1, R^2\})$  and  $Fe(CO)_5$  in solution was inferred from the IR spectra. When prolonged heating of the reaction mixture was necessary, sometimes traces of  $Fe_3(CO)_{12}$  could also be

TABLE I

ELEMENTAL ANALYSES AND FD-MASS SPECTROMETRIC DATA FOR  $M_2(CO)_6(R-Pyca)$  COMPOUNDS

Com- pound	M	Ligand substituents			Elemental analyses (Found (calcd. (%))			Mass found (calcd.)	Yield (%)
		R <sup>1</sup>	R	R <sup>2</sup>	C	H	N		
I	Fe	H	t-Bu	H	43.61 (43.48)	3.61 (3.19)	5.92 (6.34)	442 (441.99)	72
II	Fe	H	i-Pr	H	42.07 (42.10)	2.99 (2.83)	6.49 (6.55)	429 (427.96)	75
III	Fe	H	c-Hex	H	46.16 (46.19)	3.53 (3.45)	5.93 (5.99)	468 (468.02)	36
IV	Fe	H	i-Bu	H	42.98 (43.48)	3.16 (3.19)	6.25 (6.34)	442 (441.99)	68
V	Fe	H	<i>p</i> -Tol	H	45.39 (47.94)	2.43 (2.54)	4.33 (5.88)	476 (476.01)	36
VI	Fe	H	2,4,6-Mes	H	47.80 (48.82)	3.29 (3.28)	5.13 (5.69)	504 (504.06)	23
VII	Fe	Me	t-Bu	H	42.27 (44.78)	3.60 (3.54)	5.19 (6.14)	456 (456.01)	26
VIII	Fe	Me	i-Pr	H	44.01 (43.48)	3.46 (3.19)	6.13 (6.34)	442 (441.99)	64
IX	Fe	Me	c-Hex	H	46.70 (47.34)	4.02 (3.76)	5.86 (5.81)	482 (482.05)	21
X	Fe	Me	i-Bu	H	42.27 (44.78)	3.76 (3.54)	4.79 (6.14)	456 (456.01)	78
XI	Fe	Me	<i>p</i> -Tol	H	44.89 (49.02)	2.58 (2.88)	5.76 (5.72)	490 (490.03)	28
XII	Fe	H	2,4,6-Mes	H	50.24 (49.84)	3.48 (3.59)	5.35 (5.54)	518 (518.08)	26
XIII	Fe	H	c-Hex	Me	46.94 (47.34)	3.94 (3.76)	5.62 (5.81)	482 (482.05)	11
XIV	Ru	H	t-Bu	H	35.74 (36.09)	3.61 (2.65)	5.17 (5.26)	534 (532.43)	50-70
XV	Ru	H	i-Pr	H	34.46 (34.75)	2.29 (2.33)	5.24 (5.40)	519 (518.40)	50-70
XVI	Ru	H	c-Hex	H	38.34 (38.71)	2.87 (2.89)	4.88 (5.02)	558 (558.47)	50-70
XVII	Ru	Me	t-Bu	H	35.79 (37.37)	2.92 (2.95)	4.43 (5.13)	547 (546.46)	50
XVIII	Ru	Me	i-Pr	H	35.66 (36.09)	2.65 (2.65)	4.89 (5.26)	534 (532.43)	50
XIX	Ru	Me	c-Hex	H	39.70 (39.86)	3.18 (3.17)	4.98 (4.89)	573 (572.50)	50
XX	Ru	H	c-Hex	Me	40.69 (39.86)	3.93 (3.17)	4.65 (4.89)	576 (572.50)	35

detected. Separation of these species from the dinuclear  $Fe_2(CO)_6(R-Pyca)$  complex was achieved by stirring the mixture in air, which destroyed the air-sensitive, mononuclear  $Fe(CO)_3(R-Pyca)$  complex. Solvent and  $Fe(CO)_5$  were removed by evaporation at low pressure, and the residue was dissolved in  $CH_2Cl_2$  and filtered through a clay-silica-clay sandwich layer. The filtrate was concentrated, and in most cases the residue was recrystallized from hexane at  $-70^\circ C$ . The yields of the

red-brown crystalline products (Table 1) varied between 10 to 80% (isolated product) depending on the type of ligand.

*Preparation of  $Ru_2(CO)_6(R-Pyca\{R^1, R^2\})$  ( $R^1 = H, Me; R^2 = H; R = t-Bu; i-Pr, c-Hex$ )*

$Ru_3(CO)_{12}$  (0.5 mmol) was stirred for 0.5 h in 40 ml of n-heptane at 80°C. Subsequently a solution of the pyridine-imine ligand (0.75 mmol) in 10 ml of n-heptane was added dropwise during 0.5 h. The mixture was kept at 80°C for another 0.5 h, then the n-heptane was evaporated under vacuum and the residue was dissolved in n-hexane and chromatographed on a silica-gel column with n-hexane as eluent. The fraction containing the dinuclear product was concentrated and the residue then crystallized from n-hexane at -70°C, to give yellow crystals (50–70% yield; Table 1).

*Preparation of  $Ru_2(CO)_5(i-Pr-APE)$  ( $i-Pr-APE = 1,2-bis(\mu-isopropylamido)-1,2-bis(2-pyridyl)ethane$ )*

$Ru_3(CO)_{12}$  (0.5 mmol) and *i-Pr-Pyca* (1.5 mmol) were refluxed in 50 ml of toluene. After 3 h the toluene was evaporated under vacuum. The solid residue was washed with n-hexane to remove unreacted  $Ru_2(CO)_6(i-Pr-Pyca)$  and then chromatographed on a silica gel column using  $CH_2Cl_2$  as an eluent. The pure product was precipitated from the concentrated  $CH_2Cl_2$  solution by adding n-pentane and was obtained as an orange powder in 75% yield, which was recrystallized from a  $CH_2Cl_2$ /diethyl ether mixture (1/1 v/v) to give a crystalline product.

*Reactions of  $Fe_2(CO)_6(R-Pyca\{R^1, R^2\})$  ( $R^1 = H, Me; R^2 = H; R = t-Bu, i-Pr, c-Hex, i-Bu, p-Tol, 2,4,6-Mes$ )*

Attempts to prepare the Fe analogues of the  $Ru_2(CO)_5(R-APE)$  compounds under similar circumstances failed. In all cases only  $Fe(CO)_3(Pyca)$  was formed, as shown by the IR spectra of the reaction solutions.

*Data collection and refinement of  $Ru_2(CO)_5(i-Pr-APE)$  ( $C_{23}H_{24}N_4O_5Ru_2$ )*

Crystals of the title compound are monoclinic, space group  $P2/n$  with two molecules in a unit cell of dimensions  $a$  14.499(5),  $b$  9.051(3),  $c$  9.772(4) Å and  $\beta$  103.54(4)°. 1743 intensities with  $I > 2.5\sigma(I)$  were measured on a Nonius CAD 4 diffractometer using graphite monochromatic  $Cu-K\alpha$  radiation. An absorption correction was applied ( $\mu$  101.0  $cm^{-1}$ ; crystal dimensions 0.20 × 0.044 × 0.20 mm). The molecules are situated at crystallographic twofold axes. The Ru positions were derived from an  $E^2$ -Patterson synthesis. There were difficulties in interpreting the subsequent  $F_0$ -synthesis, apparently because of disorder; the molecular sites are occupied by molecules of two enantiomorphic configurations in a ratio of about 0.6/0.4. At each site the two enantiomorphs coincide except for the pyridine rings, which are in alternate *anti*-configurations about the bond C(7)–C(7\*). Anisotropic block-diagonal least-squares refinement with two fractional atoms for each of the ring atoms resulted in an  $R$  value of 0.061. The bond lengths and angles involving the ring atoms, however, were unsatisfactory owing to mutual overlap of the two fractional rings. The individual ring atoms were therefore replaced by rigid rings of ideal geometry and the refinement was repeated with two fractional rigid rings A and B with variable population parameters and overall isotropic temperature parameters. Refinement then converged to  $R = 0.057$ .

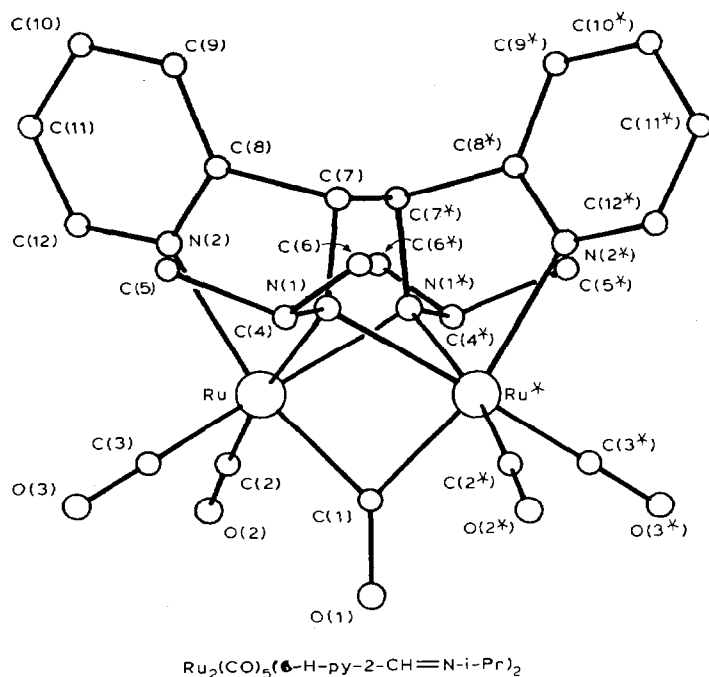
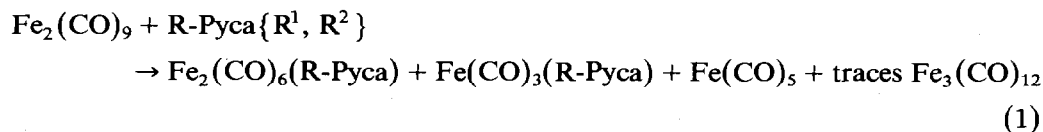


Fig. 3. Molecular geometry of  $\text{Ru}_2(\text{CO})_5(\text{i-Pr-APE})$  (Pyridine ring A, see refinement).

The atomic coordinates of Table 3 refer to this refinement\*. The unusually long bond  $\text{C}(7)\text{--}\text{C}(8)$  (1.71(2) Å) and the small angle  $\text{C}(7^*)\text{--}\text{C}(7)\text{--}\text{C}(8)$  ( $90.9(8)^\circ$ ) indicate that refinement was not complete. The part of the structure without the pyridine rings does not seem to be very much affected by the disorder, although the anisotropic temperature parameters suggest that in this part of the structure the coincidence of the two enantiomorphs is not perfect.

## Results

Thermal reactions of  $\text{Fe}_2(\text{CO})_9$  with  $\text{R-Pyca}\{\text{R}^1, \text{R}^2\}$  produce  $\text{Fe}_2(\text{CO})_6(\text{R-Pyca})$  along with  $[\text{Fe}(\text{CO})_3(\text{R-Pyca})]$ ,  $\text{Fe}(\text{CO})_5$  and sometimes also traces of  $\text{Fe}_3(\text{CO})_{12}$ , as indicated by the IR spectra of the reaction mixtures (see eq. 1).



The stoichiometry as well as the composition of these dinuclear compounds was established by elemental analyses and FD mass spectrometry (see Table 1). The yields of the dinuclear species depend strongly on the type of ligand used. In general it appears that the yields of I–XIII are somewhat lower for the ligand with  $6\text{-R}^1 = \text{Me}$  than for that having  $6\text{-R}^1 = \text{H}$  (i.e. in which there is no *ortho*-substituent),

\* Tables of thermal parameters and structure factors are available from the authors.

TABLE 2  
SOME SELECTED GEOMETRIC DATA FOR  $\text{Ru}_2(\text{CO})_5(\text{i-Pr-APE})^a$

<i>The metal-carbonyl part</i>			
Ru-Ru*	2.858(2)	Ru-C(1)-Ru*	91.8(5)
Ru-C(1)	1.989(8)	C(1)-Ru-C(2)	92.1(4)
Ru-C(2)	1.859(11)	C(1)-Ru-C(3)	92.3(4)
Ru-C(3)	1.834(10)	C(2)-Ru-C(3)	87.8(5)
C(1)-O(1)	1.241(13)	Ru-C(1)-O(1)	134.1(2)
C(2)-O(2)	1.159(15)	Ru-C(2)-O(2)	177.6(9)
C(3)-O(3)	1.170(13)	Ru-C(3)-O(3)	178.6(11)
<i>The metal-ligand part</i>			
Ru-N(1)	2.166(6)	C(1)-Ru-N(1)	83.9(3)
Ru*-N(1)	2.206(6)	C(2)-Ru-N(1)	169.9(3)
Ru-N(2)	2.249(8)	C(3)-Ru-N(1)	101.6(4)
Ru-N(2)B	2.232(8)	C(1)-Ru-N(2)	163.7(2)
		C(1)-Ru-N(2)B	164.1(2)
Ru-N(1)-Ru*	81.6(2)	C(2)-Ru-N(2)	102.0(3)
Ru*-Ru-N(1)	49.8(2)	C(2)-Ru-N(2)B	95.7(3)
Ru*-Ru-N(2)	120.1(1)	C(3)-Ru-N(2)	96.3(3)
Ru*-Ru-N(2)B	120.6(1)	C(3)-Ru-N(2)B	101.8(3)
N(1)-Ru-N(2)	80.9(2)	Ru-N(1)-C(4)	123.2(5)
N(1)-Ru-N(2)B	86.1(2)	Ru-N(1)-C(7)	105.7(5)
		Ru-N(2)-C(8)	110.4(1)
<i>The ligand part</i>			
N(1)-C(4)	1.484(10)	N(1)-C(7)-C(8)	107.7(7)
N(1)-C(7)	1.485(10)	N(2)-C(8)-C(7)	115.9(3)
N(2)-C(8)	1.349(1)	C(4)-N(1)-C(7)	113.9(6)
C(7)-C(8)	1.706(13)	N(1)-C(4)-C(5)	112.0(8)
C(4)-C(5)	1.553(16)	N(1)-C(4)-C(6)	112.9(8)
C(4)-C(6)	1.532(16)	C(5)-C(4)-C(6)	108.2(9)

<sup>a</sup> Bond distances (e.s.d.) in Å; bond angles (e.s.d.) in degrees (Pyridine ring A atoms, unless otherwise specified, see Experimental).

indicating a steric influence on the reaction course. Furthermore, it is apparent that when R (on the imine-N) is an aryl group the yield is generally much lower than when R = alkyl. Finally, when R<sup>2</sup> = Me instead of H the dinuclear compound is formed slowly and in only very low yield.

Frühauf [16] has previously reported the preparation of the complexes  $\text{Fe}_2(\text{CO})_6(\text{R-Pyca}\{\text{R}^1, \text{R}^2\})$  with R<sup>1</sup> = H; R<sup>2</sup> = H; CH<sub>3</sub> and R = n-Bu, Ph. Their IR spectra in the  $\nu(\text{CO})$  region agree with those of our dinuclear complexes. The 6  $\nu(\text{CO})$  frequencies for all the complexes lie in the expected regions [2], e.g. 2050, 2000, 1985, 1970, 1950, 1940 cm<sup>-1</sup> for  $\text{Fe}_2(\text{CO})_6(\text{Pyca})$  and 2065, 2025, 1990, 1980, 1960, 1955 cm<sup>-1</sup> for  $\text{Ru}_2(\text{CO})_6(\text{Pyca})$ , respectively (see Table 4). Frühauf did not report NMR spectra for his complexes so no comparison with our data is possible. The yield of the complexes obtained by Frühauf decreased in the order R<sup>2</sup> = H > CH<sub>3</sub> [16], but increased when the ratio  $\text{Fe}(\text{CO})_3(\text{R-Pyca})/\text{Fe}_2(\text{CO})_9$  was decreased.

The new complexes  $\text{Ru}_2(\text{CO})_6(\text{R-Pyca}\{\text{R}^1, \text{R}^2\})$  were prepared for R<sup>1</sup> = H, Me; R<sup>2</sup> = H, Me and R = t-Bu, i-Pr and c-Hex. The dinuclear complexes can also be made for other alkyl groups (e.g. R = i-Bu), but they could not be made for



TABLE 3

ATOMIC COORDINATES FOR  $\text{Ru}_2(\text{CO})_5(\text{i-Pr-APE})$  (with e.s.d.'s in parentheses)

Atom	x	y	z
Ru	0.2890(4)	0.09598(5)	0.12865(6)
N(1)	0.1707(4)	0.2189(7)	0.1713(7)
C(1)	0.2500	-0.0569(12)	0.2500
C(2)	0.4003(8)	-0.0049(10)	0.1257(10)
C(3)	0.2324(8)	-0.0033(10)	-0.0328(11)
C(4)	0.0725(6)	0.2065(10)	0.838(10)
C(5)	0.0628(9)	0.2737(15)	-0.0651(12)
C(6)	-0.0010(7)	0.2806(14)	0.1512(14)
C(7)	0.2047(7)	0.3735(9)	0.1971(13)
O(1)	0.2500	-0.1940(9)	0.2500
O(2)	0.4683(7)	-0.0722(10)	0.1255(10)
O(3)	0.1945(8)	-0.0649(12)	-0.1359(9)
N(2)A <sup>a</sup>	0.3097	0.3104	0.0233
C(8)A <sup>a</sup>	0.2610	0.4199	0.0682
C(9)A <sup>a</sup>	0.2615	0.5627	0.0160
C(10)A <sup>a</sup>	0.3133	0.5920	-0.0839
C(11)A <sup>a</sup>	0.3637	0.4784	-0.1295
C(12)A <sup>a</sup>	0.3602	0.3377	-0.0736
N(2)B <sup>b</sup>	0.3315	0.3075	0.0431
C(8)B <sup>b</sup>	0.3327	0.4154	0.1386
C(9)B <sup>b</sup>	0.3602	0.5584	0.1146
C(10)B <sup>b</sup>	0.3851	0.4775	-0.1078
C(11)B <sup>b</sup>	0.3866	0.5895	-0.0101
C(12)B <sup>b</sup>	0.3570	0.3365	-0.0783

<sup>a</sup> Refined as rigid group; fraction of pyridine ring atoms used in the refinement, 0.6, overall isotropic temperature parameter,  $0.050 \text{ \AA}^2$ . <sup>b</sup> Refined as rigid group; fraction of pyridine ring atoms used in the refinement, 0.4, applied overall isotropic temperature parameter,  $0.056 \text{ \AA}^2$ .

$\text{R}^1$  = aryl, and were obtained in only very low yields for  $\text{R}^2$  = Me and R = alkyl. Comparison of these reactions with those reported earlier for  $\text{Ru}_2(\text{CO})_6(\text{R-DAB})$  and  $\text{Fe}_2(\text{CO})_6(\text{R-DAB})$  shows that the analogous iron-R-Pyca complexes can be

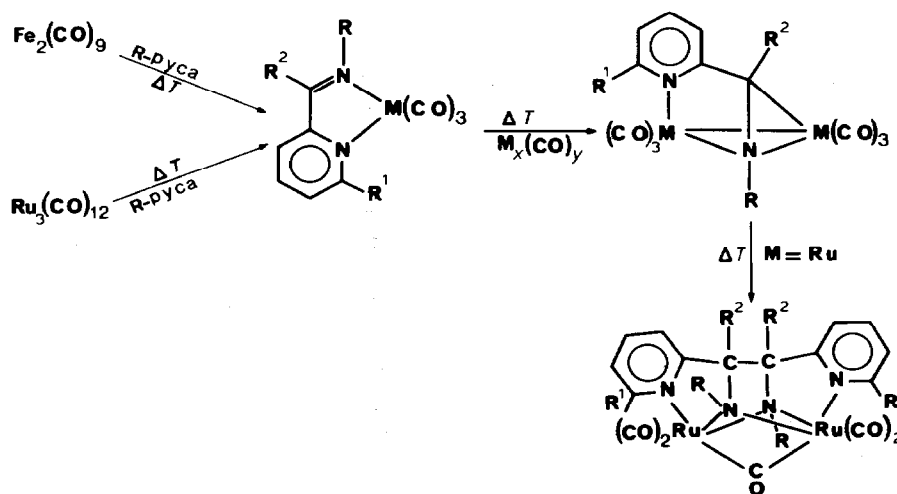
SCHEME 2. Scheme of the reactions of  $\text{Fe}_2(\text{CO})_9$  and  $\text{Ru}_3(\text{CO})_{12}$  with R-Pyca.

TABLE 4  
IR DATA FOR  $\text{Fe}_2(\text{CO})_6(\text{R-Pyca})$ ,  $\text{Ru}_2(\text{CO})_6(\text{R-Pyca})$

Compound	M	Ligand substituents			IR $\nu(\text{CO})$ values ( $\text{cm}^{-1}$ ) <sup>a</sup>					
		R <sup>1</sup>	R	R <sup>2</sup>						
I	Fe	H	t-Bu	H	2053	2003	1986	1972	1948	1943
II	Fe	H	i-Pr	H	2052	2001	1986	1970	1947	1939
III	Fe	H	c-Hex	H	2053	2003	1986	1972	1947	1940
IV	Fe	H	i-Bu	H	2052	2002	1987	1970	1947	1939
V	Fe	H	p-Tol	H	2056	2008	1987	1987	1948	1940
VI	Fe	H	2,4,6-Mes	H	2054	2008	1987	1987	1948	1940
VII	Fe	Me	t-Bu	H	2050	2002	1983	1965	1947	1939
VIII	Fe	Me	i-Pr	H	2051	2006	1983	1967	1950	1946
IX	Fe	Me	c-Hex	H	2049	2002	1982	1965	1947	1941
X	Fe	Me	i-Bu	H	2051	2004	1984	1966	1948	1942
XI	Fe	Me	p-Tol	H	2053	2006	1987	1971	1947	1940
XII	Fe	H	2,4,6-Mes	H	2051	2006	1983	1967	1950	1946
XIII	Fe	H	c-Hex	Me	2051	2000	1984	1970	1944	1937
XIV	Ru	H	t-Bu	H	2064	2025	1993	1983	1962	1956
XV	Ru	H	i-Pr	H	2065	2026	1995	1985	1964	1958
XVI	Ru	H	c-Hex	H	2064	2026	1993	1984	1961	1957
XVII	Ru	Me	t-Bu	H	2063	2023	1991	1979	1961	1955
XVIII	Ru	Me	i-Pr	H	2065	2027	1993	1982	1963	1954
XIX	Ru	Me	c-Hex	H	2066	2027	1995	1985	1963	1957
XX	Ru	H	c-Hex	Me	2068	2028	1998	1985	1964	1958

<sup>a</sup> For hexane solutions.

prepared in higher yields and more rapidly than corresponding iron-R-DAB complexes (see Schemes 1 and 2). This may be ascribed to the fact that in the case of the reactions of  $\text{Fe}_2(\text{CO})_9$  with R-DAB imidazolone derivatives and  $\text{Fe}(\text{CO})_5$  were formed, which under the reaction conditions necessary for the formation of  $\text{Fe}_2(\text{CO})_6(\text{R-DAB})$  are the major products. A similar side reaction in the  $\text{Fe}_2(\text{CO})_9/\text{R-Pyca}$  sequence is impossible because the reaction would involve loss of the resonance energy of the pyridine ring.

#### <sup>1</sup>H and <sup>13</sup>C NMR

The <sup>1</sup>H and <sup>13</sup>C NMR spectra (see Tables 5 and 6) of the compounds in  $\text{CDCl}_3$  and  $\text{C}_6\text{D}_6$  clearly show that in solution the present complexes  $\text{M}_2(\text{CO})_6(\text{R-Pyca}\{\text{R}^1, \text{R}^2\})$  ( $\text{M} = \text{Fe}, \text{Ru}$ ) have the type of structure observed for  $\text{M}_2(\text{CO})_6(\text{R-DAB})$  ( $\text{M} = \text{Fe}$  [2];  $\text{M} = \text{Ru}$  [2] and  $\text{M} = \text{Os}$  [17]). The N-donor site of the ligand is in the *E*-configuration and is  $\sigma$ -N-bonded via the pyridine moiety to  $\text{M}(1)$  (2e-donor), while the C=N part of the ligand is  $\eta^2$ -C=N bonded to  $\text{M}(2)$  (2e-donor). The N atom bridges between  $\text{M}(1)$  and  $\text{M}(2)$  and formally donates another electron pair to the dinuclear moiety (Fig. 4).

In the case of the  $\text{CR}^2$  group both the <sup>1</sup>H signal for  $\text{R}^2 = \text{H}$  and the <sup>13</sup>C signal of the imine-C atom are shifted considerably upfield with respect to values for the free ligand in the relevant solvents,  $\text{CDCl}_3$  and  $\text{C}_6\text{D}_6$  (see Tables 7 and 8).

When R is a prochiral grouping (e.g. *i*-Pr or  $\text{CH}_2\text{C}(\text{Me}_2)\text{H}$ ), the chirality of the imine-C atom in these complexes can be detected. For instance, for  $\text{R} = \text{i-Pr}$  the *i*-Pr-Me groups are diastereotopic, as shown by the observation of 2 doublets for the

(Continued on p. 367)

TABLE 5

<sup>1</sup>H NMR DATA (250 MHz) FOR M<sub>2</sub>(CO)<sub>6</sub>(R-Pyca) COMPLEXES<sup>a</sup>

Compound	Ligand substituents		Pyridine ring carbon atoms				δ(R <sup>2</sup> ) H or Me	Δ <sup>d</sup>	Substituents (R)	
	R <sup>1</sup>	R	R <sup>2</sup>	R <sup>3</sup> = H or Me	H <sup>4</sup>	H <sup>5</sup>				
I	Fe	H	H <sup>b</sup>	7.80(d)	7.38(dd)	6.96(d)	6.60(dd)	3.76(s)	4.67	1.48(s)
II	Fe	H	H <sup>b</sup>	7.76(d)	7.26(dd)	6.93(d)	6.55(dd)	3.75(s)	4.70	3.61(sept, J 6), 1.65(d), 1.55(d), (J 6)
III	Fe	H	H <sup>c</sup>	7.01(d)	6.32(dd)	6.08(d)	5.59(dd)	3.41(s)	5.11	3.00(m), (1.7-0.7)(m)
IV	Fe	H	H <sup>b</sup>	6.97(d)	6.31(dd)	6.05(d)	5.54(dd)	3.45(s)	4.78	δ(NCH <sub>2</sub> -i-Pr)diastereotopic δ(A) 4.01, δ(B) 2.97 (J <sub>AB</sub> 13, J <sub>AX</sub> 4, J <sub>BX</sub> 10), 2.43(sept), 0.77(d), 0.71(d), (J 6.6)
V	Fe	H	H <sup>c</sup>	6.99(d)	6.32(dd)	6.01(d)	5.61(dd)	3.58(s)	5.18	7.29(d, J <sub>AB</sub> 8), 6.81(d, J <sub>AB</sub> 8), 2.03(s)
VI	Fe	H	H <sup>b</sup>	7.09(d)	6.35(dd)	5.92(d)	5.62(dd)	2.95(s)	5.56	6.77(s), 6.74(s), 2.82(s), 2.08(s), 1.99(s)
VII	Fe	Me	H <sup>c</sup>	2.03(s)	6.33(dd)	6.03(d)	5.62(d)	3.63(s)	4.84	1.23(s)
VIII	Fe	Me	H <sup>c</sup>	2.00(s)	6.33(dd)	6.04(d)	5.59(d)	3.47(s)	4.95	3.27(sept, J 6), 1.32(d), 1.22(d, J 6)
IX	Fe	Me	H <sup>c</sup>	2.02(s)	6.35(dd)	6.09(d)	5.57(d)	3.56(s)	4.90	3.03(m), (2-0.9)(m)
X	Fe	Me	H <sup>c</sup>	1.98(s)	6.33(dd)	6.05(d)	5.57(d)	3.59(s)	4.84	δ(NCH <sub>2</sub> i-Pr)diastereotopic δ(A) 4.04, δ(B) 2.97 (J <sub>AB</sub> 12.9, J <sub>AX</sub> 4.2, J <sub>BX</sub> 10.4), 2.42(sept), 0.77(d), 0.71(d, J 6.6)
XI	Fe	Me	H <sup>c</sup>	2.07(s)	7.40(dd)	6.07(d)	5.70(d)	3.76(s)	5.04	7.34(d, J <sub>AB</sub> 8), 6.84(d, J <sub>AB</sub> 8), 2.03(s)
XII	Fe	Me	H <sup>c</sup>	2.03(s)	6.39(dd)	5.92(d)	5.67(d)	3.08(s)	5.39	6.76(s), 2.09(s), 2.01(s), 2.84(s)
XIII	Fe	H	Me <sup>c</sup>	7.15(d)	6.41(dd)	6.13(d)	5.63(d)	1.56(s)		3.27(m), 2.3-1(m)
XIV	Ru	H	H <sup>b</sup>	7.90(d)	7.34(dd)	7.01(d)	6.63(dd)	3.87(s)	4.56	1.32(s)
XV	Ru	H	H <sup>b</sup>	7.87(d)	7.34(dd)	7.02(d)	6.61(dd)	3.84(s)	4.61	3.12(sept, J 6), 1.43(d), 1.29(d, J 6)
XVI	Ru	H	H <sup>b</sup>	7.87(d)	7.34(dd)	7.00(d)	6.61(dd)	3.86(s)	4.61	2.63(m), (2.2-1.1, m)
XVII	Ru	Me	H <sup>b</sup>	2.53(s)	7.24(dd)	6.89(d)	6.59(d)	3.94(s)	4.36	1.31(s)
XVIII	Ru	Me	H <sup>b</sup>	2.51(s)	7.24(dd)	6.89(d)	6.58(d)	3.90(s)	4.42	3.14(sept, J 6), 1.41(d), 1.32(d, J 6)
XIX	Ru	Me	H <sup>b</sup>	2.51(s)	7.25(dd)	6.89(d)	6.58(d)	3.92(s)	4.46	2.65(m), 2.1-1.1(m)
XX <sup>c</sup>	Ru	H	Me	7.93(d)	7.42(dd)	6.95(d)	6.65(dd)	1.97(s)		3.05(m), 2-1(m)

<sup>a</sup> δ in ppm downfield from internal TMS s = singlet, d = doublet, dd = doublet of doublet, sept = septet, m = multiplet; J in Hz. <sup>b</sup> Solvent CDCl<sub>3</sub>, <sup>c</sup> Solvent C<sub>6</sub>D<sub>6</sub>.

<sup>d</sup> Δ = δ<sub>free ligand</sub> - δ<sub>metal complexes</sub>.

TABLE 6

<sup>13</sup>C NMR DATA (20.1 MHz) FOR M<sub>2</sub>(CO)<sub>6</sub>(R-Pyca) COMPLEXES<sup>a</sup>

Compound	Ligand substituents		Pyridine ring carbon atoms						$\delta(R^1)$	$\delta(R^2)$	$\Delta^d$	Substituents (R)	M-CO
	R <sup>1</sup>	R	R <sup>2</sup>	C <sup>2</sup>	C <sup>6</sup>	C <sup>3</sup>	C <sup>4</sup>	C <sup>5</sup>					
I	Fe	H	H <sup>b</sup>	173.15	151.36	136.61	118.23	116.34	64.15	91.49	60.45, 32.90	214.17	
II	Fe	H	H <sup>b</sup>	172.30	151.67	136.62	118.05	116.04	67.01	91.43	63.49, 27.08, 26.59	213.93	
III	Fe	H	c-Hex	173.17	152.17	136.75	118.37	116.36	64.48	95.56	75.95, 40.14, 39.17, 26.67	214.98	
IV	Fe	H	i-Bu	171.45	151.91	136.37	117.68	115.80	69.92	92.31	79.57, 34.66, 20.46, 19.92	214.11	
V	Fe	H	p-Tol	172.80	152.41	136.94	118.61	116.61	65.93	94.35	157.21, 136.45, 130.50, 125.83, 21.15	214.37	
VI	Fe	H	2,4,6-Mes	175.29	152.23	137.29	118.30	116.06	65.81	98.36	135.36, 136.14, 132.93, 132.02, 22.34, 20.84	219.59	
VII	Fe	Me	t-Bu	173.65	160.48	137.00	119.88	114.48	26.37	64.90	62.29, 33.22	214.74	
VIII	Fe	Me	i-Pr	173.04	160.54	137.00	119.52	114.18	26.49	67.94	65.51, 27.40, 26.85	214.86	
IX	Fe	Me	c-Hex	173.17	160.60	137.00	119.46	114.18	26.67	67.07	65.57, 40.08, 39.11, 26.67	214.86	
X	Fe	Me	i-Bu	172.01	160.79	137.12	119.28	114.12	26.51	71.70	71.70, 35.10, 20.96, 20.36	214.55	
XI	Fe	Me	p-Tol	172.30	160.40	136.92	119.26	113.86	26.59	66.34	156.46, 135.58, 129.57, 125.02, 20.70	213.08	
XII	Fe	Me	2,4,6-Mes	174.91	160.22	136.98	118.78	113.37	26.37	66.46	137.40, 138.23, 134.12, 134.01, 21.92, 20.40	215.10	
XIII	Fe	H	c-Hex	Me <sup>c</sup>	174.20	152.05	136.94	118.30	117.27	70.18	68.85, 40.38, 38.75, 26.67, 22.60(Me)	205.75	
XIV	Ru	H	t-Bu	H <sup>b</sup>	173.42	150.75	136.82	118.23	116.12	61.19	55.63, 32.63		
XV	Ru	H	i-Pr	H <sup>b</sup>	173.04	150.94	136.76	118.04	115.87	61.44	65.59, 27.46, 26.50		
XVI	Ru	H	c-Hex	H <sup>b</sup>	173.32	150.83	136.80	118.11	115.94	61.18	74.12, 41.05, 38.52, 26.85, 25.96, 23.10	196.70	
XVII	Ru	Me	t-Bu	H <sup>c</sup>	173.63	158.53	136.56	119.14	113.50	27.08	61.31, 32.48		
XVIII	Ru	Me	i-Pr	H <sup>c</sup>	173.94	159.09	137.06	119.40	113.82	27.82	66.42, 27.64, 26.91		
XIX	Ru	Me	c-Hex	H <sup>c</sup>	173.45	158.65	136.62	118.90	113.37	27.20	73.87, 40.37, 38.36, 26.23, 25.87, 22.89		
XX <sup>e</sup>	Ru	H	c-Hex	Me									

<sup>a</sup>  $\delta$  in ppm downfield from internal TMS. <sup>b</sup> Solvent CDCl<sub>3</sub>. <sup>c</sup> Solvent C<sub>6</sub>D<sub>6</sub>. <sup>d</sup>  $\Delta = \delta_{\text{free ligand}} - \delta_{\text{metal complexes}}$ . <sup>e</sup> Not measured.

TABLE 7  
<sup>1</sup>H NMR DATA (100 MHz) FOR THE PYRIDINE CARBALDEHYDE-IMINE (R-Pyca) LIGANDS<sup>a</sup>

Compound no.	Ligand substituents		Pyridine ring substituents					R <sup>2</sup> = H <sup>b</sup> or Me	R <sup>2</sup> = H <sup>c</sup> or Me	Substituent (R) <sup>b</sup>
	R <sup>1</sup>	R	R <sup>2</sup>	R <sup>1</sup> = H or CH <sub>3</sub>	H <sup>3</sup>	H <sup>4</sup>	H <sup>5</sup>			
1	H	t-Bu	H	8.65(d)	8.14(d)	7.72(br)	7.29(br)	8.43(s)	8.46(s)	1.31(s)
2	H	i-Pr	H	8.63(d)	8.05(d)	7.67(br)	7.23(br)	8.45(s)	8.48(s)	3.62(sept), 1.26(d)
3	H	c-Hex	H	8.63(d)	8.05(d)	7.67(br)	7.24(br)	8.47(s)	8.52(s)	3.32(m), (2.2-1.0)(m)
4	H	i-Bu	H	8.54(d)	7.92(d)	7.58(br)	7.14(br)	8.23(s)	8.45(s)	3.27(dd, J 6.6, J <sub>im</sub> 1.4), 1.94 (m), 0.76 (d, J 6.6)
5	H	p-Tol	H	8.71(d)	8.28(d)	7.68(br)	7.25(br)	8.67(s)	8.76(s)	7.27(s), 2.82(s)
6	H	2,4,6-Mes	H	8.70(d)	8.33(d)	7.77(br)	7.32(br)	8.42(s)	8.51(s)	6.90(s), 2.30(s), 2.18(s)
7	CH <sub>3</sub>	t-Bu	H	2.57(s)	7.75(d)	7.52(br)	7.07(d)	8.30(s)	8.47(s)	1.32(s)
8	CH <sub>3</sub>	i-Pr	H	2.53(s)	7.77(d)	7.50(br)	7.10(d)	8.32(s)	8.42(s)	3.32(sept), 1.23(d, J 6)
9	CH <sub>3</sub>	c-Hex	H	2.60(s)	7.92(d)	7.58(br)	7.23(d)	8.38(s)	8.46(s)	3.42(m), (2.2-1.0)(m)
10	CH <sub>3</sub>	i-Bu	H	2.57(s)	7.72(d)	7.45(br)	7.07(d)	8.80(s)	8.43(s)	3.14(dd, J 6.4, J <sub>im</sub> 1.3), 2.24(s), 1.70(m), 0.63 (d, J 6.7)
11	CH <sub>3</sub>	p-Tol	H	2.60(s)	7.88(d)	7.55(br)	7.17(d)	8.60(s)	8.80(s)	7.20(s), 2.35(s)
12	CH <sub>3</sub>	2,4,6-Mes	H	2.63(s)	8.06(d)	7.68(br)	7.12(d)	8.28(s)	8.47(s)	6.84(s), 2.58(s), 2.25(s), 2.11(s)
13	H	c-Hex	Me	8.52(d)	7.95(d)	7.60(br)	7.24(d)	4.37(s)	4.52(s)	5.57(m), (4-2)(m)

<sup>a</sup> δ in ppm downfield from internal TMS; s = singlet, d = doublet, dd = doublet of doublet, sept = septet, m = multiplet, br = broad; J in Hz. <sup>b</sup> Solvent CDCl<sub>3</sub>.  
<sup>c</sup> Solvent C<sub>6</sub>D<sub>6</sub>.

TABLE 8  
 $^{13}\text{C}$  NMR DATA (20.1 MHz) FOR THE PYRIDINE CARBALDEHYDE IMINE (R-Pyca) LIGANDS<sup>a</sup>

Compound no.	Ligand substituents		Pyridine ring substituents <sup>b</sup>					$\text{R}^1 = \text{CH}_3$	$\text{R}^2 = \text{H}^b$	$\text{R}^2 = \text{H}^c$	Substituents (R) <sup>b</sup>
	$\text{R}^1$	$\text{R}^2$	$\text{C}^2$	$\text{C}^6$	$\text{C}^3$	$\text{C}^4$	$\text{C}^5$				
1	H	t-Bu	154.85	148.43	135.66	123.61	120.15	155.64	156.75	57.00, 28.87	
2	H	i-Pr	154.28	148.62	135.58	123.72	120.54	158.44	159.70	60.62, 23.33	
3	H	c-Hex	154.53	148.77	135.73	123.80	120.69	158.83	160.04	68.94, 33.63, 25.11, 24.11	
4	H	i-Bu	154.58	149.04	136.03	124.14	120.74	161.47	162.23	69.08, 29.13, 26.51	
5	H	p-Tol	154.45	149.23	136.29	124.48	120.80	159.23	160.28	148.01, 136.09, 129.46, 120.76, 20.63	
6	H	2,4,6-Mes	154.28	149.20	136.21	124.79	120.71	163.08	164.17	147.59, 133.00, 128.51, 126.41, 20.36, 17.86	
7	$\text{CH}_3$	t-Bu	156.06	154.44	135.99	123.23	117.12	23.56	156.99	57.04, 28.97	
8	$\text{CH}_3$	i-Pr	157.04	153.58	135.86	123.28	117.45	23.36	158.81	60.47, 23.19	
9	$\text{CH}_3$	c-Hex	157.34	153.99	136.04	123.45	117.67	26.25	159.29	68.90, 33.65, 25.15, 24.15	
10	$\text{CH}_3$	i-Bu	157.48	153.79	136.17	123.64	117.70	29.00	161.66	69.08, 23.80, 20.21	
11	$\text{CH}_3$	p-Tol	158.23	154.18	136.61	124.46	118.72	24.22	159.88	148.39, 136.43, 129.66, 121.00, 20.87	
12	$\text{CH}_3$	2,4,6-Mes	158.19	153.98	136.63	124.66	118.08	24.16	163.57	147.88, 133.09, 128.63, 126.63, 20.56, 18.04	
13	H	c-Hex	158.07	147.69	135.68	123.34	120.61	163.14	164.12	59.75, 33.08, 25.50, 24.39, 13.13 (Me)	

<sup>a</sup>  $\delta$  in ppm downfield from internal TMS. <sup>b</sup> Solvent  $\text{CDCl}_3$ . <sup>c</sup> Solvent  $\text{C}_6\text{D}_6$ .

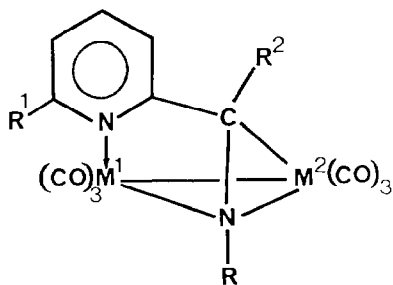


Fig. 4. Structure of  $M(1)M(2)(CO)_6(R\text{-Pyca})$  complexes ( $M = \text{Fe}$  or  $\text{Ru}$ ).

$\text{CH}_3$  protons as well as for the  $\text{CH}_3$   $^{13}\text{C}$  nuclei (see also Tables 5 and 6). A similar observation is made for the prochiral R substituents in the corresponding dinuclear ruthenium complexes.

#### *Infrared spectra ( $\nu(\text{CO})$ region)*

The  $M_2(\text{CO})_6(\text{R-Pyca})$  ( $M = \text{Fe}, \text{Ru}$ ) complexes have a  $\nu(\text{CO})$  pattern which is similar in all respects to that of  $M_2(\text{CO})_6(\text{R-DAB})$  ( $M = \text{Fe}, \text{Ru}, \text{Os}$ ) [2,17].

Neither substitution of R-DAB by R-Pyca nor the nature of the 6- $\text{R}^1$  ring substituent (H or Me) appears to have an observable effect on these values. The change from Fe to Ru gives rise to a slight increase in frequency for all the carbonyl stretching vibrations (see Table 4).

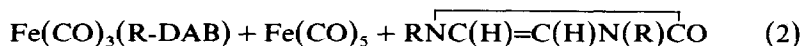
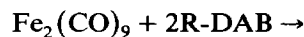
#### *Reactivity*

In reactions of  $M_2(\text{CO})_6(\text{R-Pyca})$  with R-Pyca, for  $M = \text{Fe}$  the mononuclear  $\text{Fe}(\text{CO})_3(\text{R-Pyca})$  complexes were formed; there was no trace of products originating from a C-C coupling between the two R-Pyca ligands. In the case of  $M = \text{Ru}$ , C-C coupling was observed, resulting in the formation of  $\text{Ru}_2(\text{CO})_5(\text{R-APE})$  ( $\text{R} = i\text{-Pr}$ ), starting from  $\text{Ru}_2(\text{CO})_6(\text{R-Pyca})$  and R-Pyca. These reactions and the complexes  $\text{Ru}_2(\text{CO})_n(\text{R-APE})$  ( $n = 4, 5$ ) containing the C-C linked R-Pyca ligands will be discussed in a forthcoming paper.

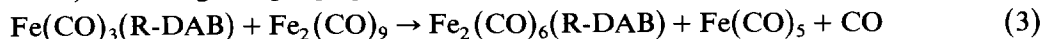
In the present publication only the structure of  $\text{Ru}_2(\text{CO})_5(\text{R-APE})$  ( $\text{R} = i\text{-Pr}$ ) is presented; this is the first unambiguous proof of the formation of a ruthenium complex containing two C-C coupled  $\alpha$ -diimines.

#### **Discussion**

It has been shown by Frühauf et al. [18], and later more quantitatively by Staal et al. [19], that  $\text{Fe}_2(\text{CO})_9$  reacts with two moles of R-DAB ( $\text{R} = t\text{-Bu}$ ) to give  $\text{Fe}(\text{CO})_3(\text{R-DAB})$ ,  $\text{Fe}(\text{CO})_5$  and imidazolone ( $\overline{\text{RNC(H)=C(H)N(R)CO}}$ ) in an exact 1/1/1 molar ratio (eq. 2). The reaction can also be brought about by using a catalytic amount of  $\text{Fe}_2(\text{CO})_9$ , in which case, however, the reaction stops after only a few cycles owing to the formation of non-productive side products, viz.  $\text{Fe}(\text{CO})_3(\text{R-DAB})$  and  $\text{Fe}(\text{CO})_5$  [19].

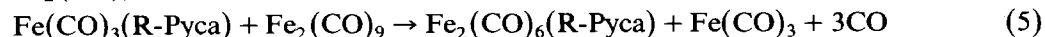
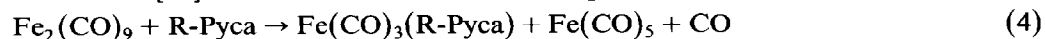


Subsequent reaction of  $\text{Fe}(\text{CO})_3(\text{R-DAB})$  with  $\text{Fe}_2(\text{CO})_9$  afforded  $\text{Fe}_2(\text{CO})_6(\text{R-DAB})$  according to eq. 3 [19].



In the analogous reactions with R-Pyca, imidazolone type of compounds were not isolated, probably because resonance stabilization of the pyridine ring blocks the formation of an unsaturated C=C bond between the two imine carbon atoms.

Frühauf [16] has shown that the formation proceeds in two steps (eqs. 4 and 5).



When the reactions were monitored with IR spectroscopy it was found that  $\text{Fe}(\text{CO})_3(\text{R-Pyca})$ , having characteristic  $\nu(\text{CO})$  values, was initially formed and then the dinuclear species  $\text{Fe}_2(\text{CO})_6(\text{R-Pyca})$  ( $\nu(\text{CO})$  2052, 2004, 1985, 1975, 1948, 1943  $\text{cm}^{-1}$ ). Thus the reaction was stopped once the carbonyl stretching IR bands of  $\text{Fe}_2(\text{CO})_6(\text{R-Pyca})$  were no longer increasing. The yield of  $\text{Fe}_2(\text{CO})_6(\text{R-Pyca}\{\text{R}^1, \text{R}^2\})$  appeared to be low when  $\text{R} = \text{Aryl}$ , and this was also the case when a methyl group was present at the imine-carbon atom ( $\text{R}^2 = \text{Me}$ ). It has previously been reported that, in a sequence analogous to that for the iron system, the reaction of  $\text{Ru}_3(\text{CO})_{12}$  with R-DAB proceeds via a prior breakdown of the trinuclear cluster to mononuclear  $\text{Ru}(\text{CO})_3(\text{R-DAB})$  complexes, after which, depending strongly on the steric properties of R, di-, tri- or tetranuclear clusters can be formed [3,4] (see Scheme 1).

The dinuclear  $\text{Ru}_2(\text{CO})_6(\text{R-DAB})$  compound is formed not only when  $\text{R} = \text{t-Bu}$ , but also when  $\text{R} = \text{i-Pr}$  and  $\text{c-Hex}$ , which demonstrates that these substituents all leave sufficient space about the diimine skeleton for a metal- $\eta^2\text{-C=N}$  bond to be formed. When, however, aryl-imine substituents are present the  $\text{Ru}_2(\text{CO})_6(\text{Aryl-DAB})$  complexes are not stable and react further via C-C coupling and decoupling routes (routes 7-9, Scheme 1) to give  $\text{Ru}_2(\text{CO})_4(\text{Aryl-DAB})_2$ : thus  $\text{Ru}_2(\text{CO})_5(\text{Aryl-IAE})$  was observed spectroscopically but could not be isolated. The observation that  $\text{Fe}_2(\text{CO})_6(\text{Aryl-Pyca})$  complexes are formed in only low yields can then be accounted for in terms of the lower basicity of the imine-N donor site for  $\text{R} = \text{Aryl}$  than for  $\text{R} = \text{Alkyl}$ ; for  $\text{R} = \text{Aryl}$  this will lead to a less effective  $\eta^2\text{-C=N}$ -iron interaction. Accordingly equilibrium 3 lies over towards the starting products. The fact that, in contrast to the impossibility of obtaining  $\text{Ru}_2(\text{CO})_6(\text{Aryl-DAB})$ , small yields of  $\text{Fe}_2(\text{CO})_6(\text{Aryl-DAB})$  can be isolated must be connected to the inhibition of the subsequent C-C(de)coupling reactions (routes 7, 8 and 9 Scheme 1) which operate in the ruthenium case.

Similar arguments apply to the observation that the yields of  $\text{Ru}_2(\text{CO})_6\text{L}$  are higher for  $\text{L} = \text{R-Pyca}$  than for  $\text{L} = \text{R-DAB}$ . In this case, also, the difficulty of forming the 8e-donor bonding between the metal and R-Pyca effectively prevents a subsequent reaction sequence similar to routes 4 and 5 in Scheme 1.

However, since the yields of  $\text{Fe}_2(\text{CO})_6(\text{R-Pyca})$  are also higher than of  $\text{Fe}_2(\text{CO})_6(\text{R-DAB})$  other factors may also be important. One factor stabilizing  $\text{Fe}_2(\text{CO})_6(\text{R-Pyca})$  may be the stronger bonding of the R-Pyca ligand with the dinuclear  $\text{Fe}_2$  unit compared with that of the R-DAB ligand. This suggestion is supported by the fact that  $\text{Ru}_2(\text{CO})_6(\text{Aryl-Pyca})$  could not be isolated from the  $\text{Ru}_3(\text{CO})_{12}$ -Aryl-Pyca reactions: further product formation via C-C coupling-decoupling reactions may have occurred (routes 7, 8 and 9, Scheme 1).



### Spectroscopic data

Since a sufficient number of complexes  $M_2(CO)_6(R-DAB)$  and  $M_2(CO)_6(R-Pyca)$  ( $M = Fe, Ru$ ) is known it appears timely to compare their IR and NMR spectroscopic data. Comparison of the Ru and Fe-R-Pyca series shows that the  $\nu(CO)$  frequencies of the Ru-R-Pyca compounds lie at somewhat higher frequencies than those of the Fe-R-Pyca compounds. A similar observation was made for the Ru- and Fe-R-DAB series [2]. This indicates more  $\pi$ -back-bonding from Fe than from Ru to the  $\pi^*-C=O$  MO (and hence also to the  $\pi^*-C=N$  MO on the  $\alpha$ -diimine), as expected on the basis of the higher lying relevant  $d$ -orbitals of Ru [20,21].

Examination of the  $^1H$  and  $^{13}C$  NMR spectral data for the free and bonded ligands shows that the pyridine resonances do not change significantly on complexation, and that substitution of the H on the 6-position by Me ( $R^1$ ) has hardly any effect. The most sensitive resonances in both the R-Pyca and R-DAB ligands are those for the imine  $^1H$  and  $^{13}C$  nuclei of the  $\eta^2$ -bonded HC=N moiety. Both the  $^1H$  and  $^{13}C$  signals (Tables 5 and 6 resp.) move strongly upfield owing to strong  $\pi$ -back-bonding from the metal atom to the  $\pi^*$ -orbital of the imine group. It is of interest to consider the values of  $\Delta$ , where  $\Delta = \delta(\text{ligand}) - \delta(\text{complex})$ , since for series of isostructural and isoelectronic complexes these may be an indicator of the measure of the  $\pi^*$ -backbonding. From the results in Tables 5 and 6 it is clear that the highest  $\Delta$  values occur for  $R = \text{Aryl}$ , which is in line with the view that the Aryl-DAB ligands are better  $\pi$ -acceptors than Alkyl-DAB ligands [22].

Within the series of Ru complexes with  $R = \text{Alkyl}$  there is little difference between t-Bu, i-Pr and c-Hex. In the Fe series the larger values for  $\Delta(^{13}C)$  and  $\Delta(^1H)$  are found for  $R = \text{c-Hex}$ , but only if  $R^1 = H$ , since for  $R^1 = \text{Me}$  the  $\Delta$  values again vary very little for the various alkyl groups. We thus conclude that the  $\Delta$  values strongly indicate that there is decreasing  $\pi$ -back-bonding in the order  $R = \text{Aryl} > \text{Alkyl}$ . Opposite trends in the  $\Delta$  values are observed when going from Fe to Ru in the respective R-Pyca and R-DAB complexes, since the  $\Delta(^1H)$  and  $\Delta(^{13}C)$  values increase in the order  $Fe > Ru$  and  $Ru > Fe$ , respectively. Since stronger  $\pi$ -back-bonding by Fe than by Ru would be expected, the  $\Delta(^1H)$  shifts may be a better indication of the measure of  $\pi$ -backbonding than the  $\Delta(^{13}C)$  values.

The only conclusion which we can draw from the spectral measurements is that the  $\pi$ -back-bonding in the Fe series decreases in the order  $R = \text{Aryl} > \text{Alkyl}$  (vide supra). The difference between R-DAB and R-Pyca in both the IR ( $\nu(CO)$  region) and in the NMR  $\Delta$  values is small and variable, indicating that there are no significant differences between R-DAB and R-Pyca in this respect, although it has been claimed that for chelated diimines R-DAB is a better  $\pi$ -acceptor than R-Pyca [22].

### Reactivity

The differences in reactivity between  $Fe_2(CO)_6(R-DAB)$  and  $Fe_2(CO)_6(R-Pyca)$  on the one hand and between  $Ru_2(CO)_6(R-DAB)$  and  $Ru_2(CO)_6(R-Pyca)$  on the other, as well as between the R-DAB and R-Pyca complexes are interesting. The iron compounds  $Fe_2(CO)_6L$ , ( $L = R-Pyca$  or R-DAB) react with R-Pyca and R-DAB to produce  $Fe(CO)_3L$ . No traces of products containing two C-C coupled  $\alpha$ -diimines have been observed. In contrast with the absence of reaction for the  $Fe_2(CO)_6(L)$  complexes, it was found that  $Ru_2(CO)_6(R-DAB)$  reacts with R-DAB via  $Ru_2(CO)_5(R-DAB)$  to give  $Ru_2(CO)_5(R-IAE)$ , which contains a R-IAE ligand

formed by coupling of two R-DAB groups [2]. Subsequent heating of  $\text{Ru}_2(\text{CO})_5(\text{R-IAE})$  then leads to elimination of one CO yielding  $\text{Ru}_2(\text{CO})_4(\text{R-IAE})$ , which contains a Ru–Ru bond. Further heating at elevated temperatures ( $120^\circ\text{C}$ ) finally causes rupture of the initially formed C–C bond to give  $\text{Ru}_2(\text{CO})_4(\text{R-DAB})_2$  (Scheme 1). It is now clear that  $\text{Ru}_2(\text{CO})_6(\text{R-Pyca})$  reacts similarly, with excess R-Pyca to give  $\text{Ru}_2(\text{CO})_5(\text{R-APE})$  for e.g.  $\text{R} = i\text{-Pr}$ ,  $\text{R}^1 = \text{H}$  or  $\text{Me}$ ,  $\text{R}^2 = \text{H}$ . This reaction probably does not involve the intermediate formation of  $\text{Ru}_2(\text{CO})_5(\text{R-Pyca})$  because the Pyca ligand cannot bind in the 8e bonding mode as discussed earlier. A detailed account of the reactions will be given in a forthcoming publication.

*Structure of  $\text{Ru}_2(\text{CO})_5(i\text{-Pr-APE})$ .* This structure is of interest because it had proved impossible to obtain suitable crystals for an X-ray structure determination in the case of  $\text{Ru}_2(\text{CO})_n(\text{R-IAE})$  ( $n = 4, 5$ ). The molecular geometry of  $\text{Ru}_2(\text{CO})_5(\text{R-APE})$  with  $\text{R} = i\text{-Pr}$  and  $\text{R}^1 = \text{R}^2 = \text{H}$  involves a well-defined  $\text{Ru}_2(\text{CO})_5$  unit bridged by a 10e donor *i*-Pr-APE ligand. Owing to disorder at the linked C centres in the APE ligand (see Fig. 3), a detailed discussion of the bond lengths and bond angles of this part of the molecule is not justified.

### Acknowledgements

We thank Mr. D. Heijdenrijk for collecting the X-ray data, Mr. R. Fokkens, Mr. R. Bregman for recording the mass spectra and Mr. J.M. Ernsting for recording the 250 MHz NMR spectra.

### References

- 1 L.H. Staal, L.H. Polm, K. Vrieze, F. Ploeger and C.H. Stam, *Inorg. Chem.*, 20 (1981) 3590.
- 2 L.H. Staal, L.H. Polm, R.W. Balk, G. van Koten, K. Vrieze and A.M.F. Brouwers, *Inorg. Chem.*, 19 (1980) 3343.
- 3 J. Keijsper, L.H. Polm, G. van Koten, K. Vrieze, G. Abbel and C.H. Stam, *Inorg. Chem.*, 23 (1984) 2142.
- 4 J. Keijsper, L.H. Polm, G. van Koten, K. Vrieze, F.A.B. Seignette and C.H. Stam, *Inorg. Chem.*, 24 (1985) 518.
- 5 L.H. Polm, J. Keijsper, M. Cluistra, G. van Koten, K. Vrieze, R.R. Andrea, K. Goubitz and C.H. Stam, to be published.
- 6 J. Keijsper, L.H. Polm, G. van Koten, K. Vrieze, C.H. Stam and J.D. Schagen, *Inorg. Chim. Acta*, 103 (1985) 137.
- 7 G. van Koten, J.T.B.H. Jastrzebski and K. Vrieze, *J. Organomet. Chem.*, 250 (1983) 49.
- 8 A. de Cian and R. Weiss, *J. Chem. Soc., Chem. Commun.*, (1976) 249.
- 9 H.W. Frühauf, F. Seils, M.J. Romao and R.J. Goddard, *Angew. Chem.*, 95 (1983) 1014.
- 10 L.H. Polm, C.J. Elsevier, G. van Koten, K. Vrieze, R.R. Andrea and C.H. Stam, to be published.
- 11 L.H. Staal, G. van Koten, R.H. Fokkens and N.M.M. Nibbering, *Inorg. Chim. Acta*, 50 (1981) 205 and references therein.
- 12 E. Speyer and H. Wolf, *Chem. Ber.*, 60 (1927) 1424.
- 13 G. Bähr and H. Thämlitz, *Z. Anorg. Allg. Chem.*, 282 (1955) 3.
- 14 G. Bähr and H.G. Döge, *Z. Anorg. Allg. Chem.*, 292 (1957) 119.
- 15 M.A. Robinson, J.D. Curry and D.H. Busch, *Inorg. Chem.*, 6 (1963) 1178.
- 16 H.W. Frühauf, *Habilitationsschrift, Univ./Gesamthochschule Duisburg* 1980.
- 17 L.H. Staal, G. van Koten and K. Vrieze, *J. Organomet. Chem.*, 206 (1981) 99.
- 18 H.W. Frühauf, A. Landers, R. Goddard and C. Krüger, *Angew. Chem.*, 90 (1978) 56.
- 19 L.H. Staal, L.H. Polm and K. Vrieze, *Inorg. Chim. Acta*, 40 (1980) 165.
- 20 M.W. Kokkes, D.J. Stufkens and A. Oskam, *J. Chem. Soc., Dalton Trans.*, (1983) 439.
- 21 R.R. Andrea, J.N. Louwen, M.W. Kokkes, D.J. Stufkens and A. Oskam, *J. Organomet. Chem.*, 281 (1985) 273.
- 22 J. Reinhold, R. Benedix, P. Birner and H. Hennig, *Inorg. Chim. Acta*, 33 (1979) 209.